

Macrocyclic Di- and Tetranuclear Osmacycloferrocenophanes^{†,1}

Ekkehard Lindner,* Christoph S. Ayasse, Klaus Eichele, and Manfred Steimann

Universität Tübingen, Institut für Anorganische Chemie, Auf der Morgenstelle 18,
72076 Tübingen, Germany

Received April 18, 2002

The novel dinuclear and tetranuclear *ortho*-, *meta*-, and *para*-osmacycloferrocenophanes [η^5 -C₅H₄(CH₂)_{*n*}-1,*m*-C₆H₄(CH₂)_{*n*}Os(CO)₄(CH₂)_{*n*}-1,*m*-C₆H₄(CH₂)_{*n*}C₅H₄- η^5]_{*x*}Fe_{*x*} (*n* = 2–4, *m* = 2–4; *x* = 1: **3a–h**; *x* = 2: **4a–h**) have been made available by the reaction of the corresponding bis(triflates) [η^5 -C₅H₄(CH₂)_{*n*}-1,*m*-C₆H₄(CH₂)_{*n*}OTf]₂Fe (**2a–h**) with Na₂[Os(CO)₄] in refluxing dimethyl ether. The macrocycles of **3b,c,e** and **4a,h** were investigated by X-ray structural analyses and consist of an extended hydrocarbon skeleton containing additionally two and four transition metal centers, respectively. In the case of the dinuclear osmacycloferrocenophanes **3a–h** the redox behavior was examined by means of cyclic voltammetry, and the results were compared with those of the bis(alcohols) **1a–h**, which were used as starting compounds for the bis(triflates) **2a–h**. With increasing chain length the ferrocene unit is easier oxidized, and in the case of **3f–h** the *E*_{1/2} values are in the region of diethylferrocene.

Introduction

Cyclophanes² with subgroups such as calixarenes³ or cryptophanes⁴ and other macromolecules of this type play an important role in the development of supramolecular chemistry,⁵ now expanding to supramolecular science,⁶ a multidisciplinary field. Soon after the discovery of ferrocene⁷ in the early 1950s and the discovery of its extraordinary features such as aromaticity, thermal stability, and resistance to aerial oxygen, interest has focused on bridged ferrocenes, denoted as ferrocenophanes.⁸ The collective term of metallocenophanes and cyclophanes is “phanes”.⁹ Replacing methylene groups of the bridging chains in these macrocycles by transition metals affords metallametalocenophanes¹⁰ and metallacyclophanes.¹¹ Due to the steric requirement

of transition metal fragments, their introduction into the framework of these systems affects the geometric parameters of the cavities.^{11,12} Simultaneously a new reactive center is obtained that is capable of inserting small molecules, like carbon monoxide,^{11a,b} into metal–carbon σ bonds and of reacting with a new ligand if a vacant coordination site is available.¹³ With the incorporation of coordination chemistry into supramolecular chemistry self-assembly¹⁴ resulted in a breakthrough in the field of molecular manufacturing of molecular polygons and polyhedra. The specific integration of heteroatoms (N, O, S) into the framework of cyclophanes or metallocenophanes leads to systems with particular complexation abilities suitable for molecular recognition.¹⁵ Considerable chemical and physical properties are expected if additional metals are in the proximity of the redox active ferrocene unit.¹⁶

With the intention to merge osmacyclophanes¹¹ and osmaferrocenophanes,¹⁰ the objective of this investigation was the synthesis of the two-dimensional osmacycloferrocenophanes **3a–h** and diosmacycloferrocenophanes **4a–h** containing two and four transition metal centers, respectively. These macrocycles differ in the

[†] Dedicated to Professor Wolfgang Beck on the occasion of his 70th birthday.

* To whom correspondence should be sent. E-mail: ekkehard.lindner@uni-tuebingen.de.

(1) Preparation, Properties, and Reactions of Metal-Containing Heterocycles. Part 107. Part 106: Lindner, E.; Khanfar, M. *J. Organomet. Chem.* **2001**, *630*, 244.

(2) (a) Vögtle, F. *Cyclophan-Chemie*; Teubner: Stuttgart, 1990. (b) Diederich, F. *Cyclophanes*; The Royal Society of Chemistry: Cambridge, 1991. (c) Vögtle, F.; Seel, C.; Windscheif, P.-M. In *Comprehensive Supramolecular Chemistry*; Atwood, J. L., Davies, J. E. D., MacNicol, D. D., Vögtle, F., Lehn, J. M., Eds.; Pergamon: Oxford, 1996; Vol. 2, p 211.

(3) (a) Ikeda, A.; Shinkai, S. *Chem. Rev.* **1997**, *97*, 1713. (b) Rebek, J., Jr. *Chem. Commun.* **2000**, 637. (c) Ibach, S.; Prautzsch, V.; Vögtle, F.; Chartroux, C.; Gloe, K. *Acc. Chem. Res.* **1999**, *32*, 729.

(4) Collet, A. In *Comprehensive Supramolecular Chemistry*; Atwood, J. L., Davies, J. E. D., MacNicol, D. D., Vögtle, F., Lehn, J. M., Eds.; Pergamon: Oxford, 1996; Vol. 2, p 325.

(5) Lehn, J.-M. *Supramolecular Chemistry*; VCH: Weinheim, 1995. (6) Reinhoudt, D. N.; Stoddart, J. F.; Ungaro, R. *Chem. Eur. J.* **1998**, *4*, 1349.

(7) Long, N. J. *Metallocenes*; Blackwell Science: Oxford, 1998.

(8) (a) Mueller-Westerhoff, U. T. *Angew. Chem., Int. Ed. Engl.* **1986**, *25*, 702. (b) Heo, R. W.; Lee, T. R. *J. Organomet. Chem.* **1999**, *578*, 31.

(9) Vögtle, F.; Neumann, P. *Tetrahedron* **1970**, *26*, 5847.

(10) Lindner, E.; Krebs, I.; Fawzi, R.; Steimann, M.; Speiser, B. *Organometallics* **1999**, *18*, 480.

(11) (a) Lindner, E.; Pitsch, M. W.; Fawzi, R.; Steimann, M. *Chem. Ber.* **1996**, *129*, 639. (b) Lindner, E.; Wassing, W.; Pitsch, M. W.; Fawzi, R.; Steimann, M. *Inorg. Chim. Acta* **1994**, *220*, 107. (c) Lindner, E.; Wassing, W.; Fawzi, R.; Steimann, M. *Angew. Chem., Int. Ed. Engl.* **1994**, *33*, 321.

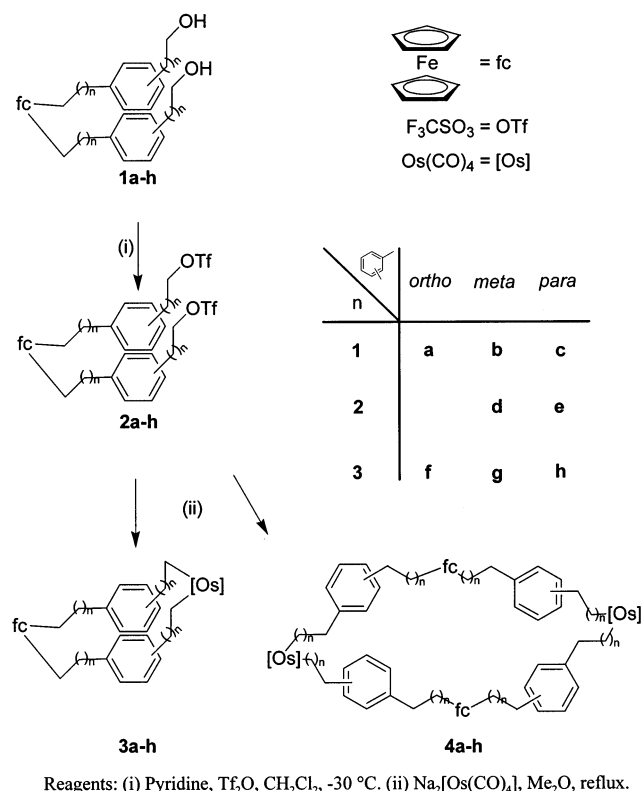
(12) Jones, C. J. *Chem. Soc. Rev.* **1998**, *27*, 289. (13) Holliday, B. J.; Mirkin, C. A. *Angew. Chem., Int. Ed.* **2001**, *40*, 2022.

(14) (a) Stang, P. J.; Olenyuk, B. *Acc. Chem. Res.* **1997**, *30*, 502. (b) Leininger, S.; Olenyuk, B.; Stang, P. J. *Chem. Rev.* **2000**, *100*, 853. (c) Fujita, M.; Umemoto, K.; Yoshizawa, M.; Fujita, N.; Kusakawa, T.; Biradha, K. *Chem. Commun.* **2001**, 509.

(15) Weber, E.; Vögtle, F. In *Comprehensive Supramolecular Chemistry*; Atwood, J. L., Davies, J. E. D., MacNicol, D. D., Vögtle, F., Lehn, J.-M., Eds.; Pergamon: Oxford, 1996; Vol. 2, p 1.

(16) Barlow, S.; O'Hare, D. *Chem. Rev.* **1997**, *97*, 637.

Scheme 1



lengths of the alkyl chains and the different substitution patterns at the aromatic rings. The well-known bis(triflate) method^{10,11,17} served for the formation of two and four osmium–carbon σ bonds, respectively. The redox potentials of **3a–h** were determined by cyclic voltammetry and were dependent on the chain lengths and substitution design. Selected osmacycloferrocenophanes and diosmacycloferrocenophanes were subjected to an X-ray structural investigation.

Results and Discussion

For the synthesis of the osmacycloferrocenophanes **3** and **4** according to Scheme 1, advantage of the bis(triflate) method was taken, which is considered as a variant of the cationic alkylation. This route was found to be the most straightforward and efficient way for the concomitant formation of several metal–carbon σ bonds under very mild conditions. The triflate residue is an excellent and inert leaving group, stabilizing carbenium-like carbon atoms at the ends of a hydrocarbon chain, thereby enabling an electrophilic attack of the terminal carbon atoms even at a weakly basic metal center. With regard to this method metallacyclophanes¹¹ and four-¹⁸ to 51-membered¹⁹ multimetallacycloalkanes were obtained by reaction of the corresponding bis(triflates) with the metalates $[M(CO)_4]^{2-}$ ($M = Fe, Ru, Os$). Prior to the application of the bis(triflate) method in this work several primary steps had to be elaborated.

Synthesis of the Bis(triflates) 2a–h. Due to the unavailability of the symmetrical ferrocenediyl alcohols

1a–h (Scheme 1), several starting materials had to be made accessible (see also Supporting Information). Treatment of the tetrahydropyran (THP)-protected cyclopentadienyl alcohols with $FeCl_2(THF)_{1.44}$ ²⁰ in THF with subsequent deprotection of the resulting intermediates affords the bis(alcohols) **1a–h**. After purification by column chromatography **1a–h** were obtained in moderate to satisfying yields. While the *para*-compounds **1c,h** represent orange waxy solids, the bis(alcohols) **1a,b,d–g** are highly viscous yellow oils. All alcohols **1a–h** are readily soluble in chlorinated hydrocarbons, and their molecular composition was corroborated by elemental analyses and FD mass spectra, displaying in each case the expected molecular peak.

To attain the bis(triflates) **2a–h** in good to excellent yields, the bis(alcohols) **1a–h** were reacted with trifluoromethanesulfonic acid anhydride in the presence of a slight excess of pyridine at $-30\text{ }^\circ\text{C}$ in dichloromethane. The yellow, heat-sensitive compounds **2a–h** are easily soluble in common organic solvents and can be stored below $-30\text{ }^\circ\text{C}$ for some days. However, it is recommendable to use them in situ. **2a–h** were identified by their mass, 1H , $^{13}C\{^1H\}$ NMR, and IR spectra (see Supporting Information).

Synthesis and Characterization of the Osmacycloferrocenophanes 3a–h. The osmacycloferrocenophanes **3a–h** were formed within 3 days in satisfying yields by adding the corresponding bis(triflates) **2a–h** to a suspension of the sodium salt of the organometallic Lewis base $[Os(CO)_4]^{2-}$ in refluxing dimethyl ether (Scheme 1). Because of the low solubility of $Na_2[Os(CO)_4]$ in this solvent, the necessary dilution was adjusted automatically; hence the formation of oligo- and polymeric products was suppressed as far as possible. A yellow-brown precipitate consists of mainly oligomers, polymers, and sodium triflate. For the macrocycles **3a–h** with longer alkyl chains a trend to higher yields was observed. The yellow osmacycloferrocenophanes **3a–h** (Chart 1) are rather stable toward aerial oxygen, can be handled at room temperature without decomposition, and dissolve in all common organic solvents. Their molecular composition was confirmed by elemental analyses and by FD mass spectra, displaying in each case the expected isotopic pattern. Between 2130 and 2000 cm^{-1} the IR spectra of **3a–h** exhibit three to four CO absorptions (*n*-pentane), which together with their intensities is consistent with the presence of *cis*- $Os(CO)_4$ arrangements.

By inspection of the 1H and $^{13}C\{^1H\}$ NMR spectra it is obvious that most chemical shifts remain largely unchanged on going from the ferrocenediyl alcohols **1a–h** to the macrocycles **3a–h** via the bis(triflates) **2a–h**. For the aromatic protons in **1a–h**, **2a–h**, and **3a–h** the centers of the chemical shifts are located between 7.22 and 7.04 ppm. If the 1H NMR spectra of **3c**, **3e**, and **3h** are compared in the aromatic region, a particular conspicuous dependence of the splitting pattern on the length of the *para*-positioned alkyl chain appears, revealing an AA'BB' system for **3c** collapsing into a singlet on going from **3c** to **3e** and **3h**. In **3h** the different functional groups are too far away from the

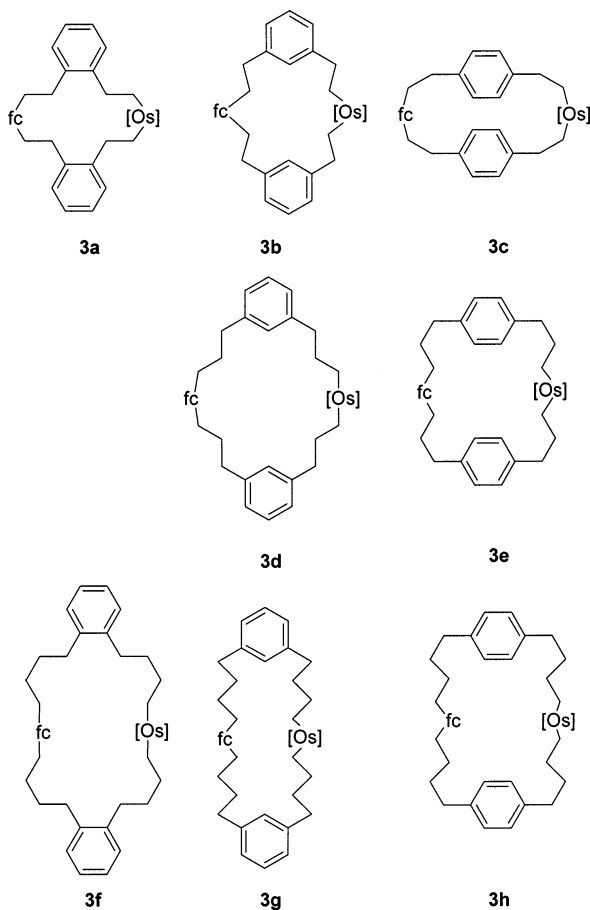
(17) Lindner, E.; Au, G.; Eberle, H.-J. *Chem. Ber.* **1981**, *114*, 810.

(18) Lindner, E.; Jansen, R. M.; Hiller, W.; Fawzi, R. *Chem. Ber.* **1989**, *122*, 1403.

(19) Linder, E.; Leibfritz, T.; Fawzi, R.; Steimann, M. *Chem. Ber.* **1997**, *130*, 347.

(20) *Synthetic Methods of Organometallic and Inorganic Chemistry*; Hermann, W. A., Ed.; Georg Thieme Verlag: Stuttgart, 1996; Vol. 1, p 135.

Chart 1



benzene ring. While the spectra of **3a–h** show AA'XX' patterns for the cyclopentadienyl hydrogen atoms in the case of the bis(alcohols) **1a–h** and bis(triflates) **2a–h**, only a broad singlet or a diffuse AA'XX' spin system occurs. All centers of chemical shifts are found in the range between 4.09 and 3.87 ppm. The multiplets (2.9–2.29 ppm) of the four CH₂ groups adjacent to the aromatic rings in the ¹H NMR spectra of **1a–h**, **2f–h**, and **3b,d–h** are not resolved. Only for **2a–e** and **3a,c** are separated signals for these functions observed. On the contrary, the resonances of the protons of the methylene groups next to the ferrocene unit in **1d–h**, **2d–h**, and **3d–h** are relatively constant (2.37–2.25 ppm) and give rise to triplets. All other spectra (**1a–c**, **2a–c**, **3a–c**) show only unresolved multiplets (2.74–2.12 ppm). Depending on the electron-donating or electron-withdrawing properties of the respective functions, the largest chemical shift differences are detectable for the protons of the methylene groups in direct vicinity to Os(CO)₄ (1.41–0.94 ppm), OH (3.83–3.56 ppm), and OTf (4.74–4.55 ppm). Except **3c,h**, with a hindered rotation of the C_α–C_β bonds (with respect to osmium), the spectra of the osmacycloferrocenophanes **3a,b,d–f,g** reveal the same splitting pattern²¹ for the CH₂Os groups. For example in the case of **1b** the A (CH₂–Ar) and X (CH₂Os) parts of the AA'XX' spin system are characterized by chemical shifts of 3.03 and 1.40 ppm, respectively. The protons of the internal methylene groups between the aromatic rings and the ferrocene

Table 1. Selected Bond Lengths (Å) and Bond Angles (deg) for **3b**, **3c**, and **3e**

	3b	3c	3e
Os(1)–Fe(1)	8.139(2)	9.727(2)	11.468(3)
Os(1)–C(5)	2.221(4)	2.220(7)	2.203(5)
Os(1)–C(20)	2.229(4)	2.236(7)	
Os(1)–C(22)			2.219(20)
center Ph(1)–center Ph(2)	8.41	5.58	6.52
Fe–Cp(1)	1.65	1.66	1.65
Fe–Cp(2)	1.65	1.66	1.64
C(5)–Os(1)–C(20)	83.66(16)	82.8(3)	
C(5)–Os(1)–C(22)			83.69(18)
δ	178.1	177.9	178.2
α	2.31(32)	3.77(41)	2.17(30)
C(14)–Cp(1)–Cp(2)–C(29)	66.3	0.1	
C(16)–Cp(1)–Cp(2)–C(33)			62.3
interplanar angle (Ph(1)–Ph(2))	82.29(14)	53.73(17)	27.99(24)

and Os(CO)₄, OTf, or OH groups, respectively, give rise only to unresolved multiplets between 2.1 and 1.6 ppm.

Like in the ¹H NMR spectra the largest differences of the chemical shifts in the ¹³C{¹H} NMR spectra of **1a–h**, **2a–h**, and **3a–h** are ascertained for the carbon atoms of the CH₂ functions next to Os, OH, and OTf. The ranges of the ¹³C resonances vary from 1.8 to –5.5 (CH₂Os), 63.7 to 62.2 (CH₂OH), and 78.1 to 77.3 ppm (CH₂OTf), respectively. Unlike previous results,^{10,19} the high-field position of the α-methylene carbon atoms in the spectra of the osmacycloferrocenophanes **3a–h** exhibit no significant dependence on the ring size. All other methylene groups (three for **Xa–c**, five for **Xd,e**, seven for **Xf–h**, X = 1–3) resonate between 43.6 and 26.7 ppm. Three signals between 91 and 67 ppm are assigned to the cyclopentadienyl carbon atoms in the spectra of **1a–h** to **3a–h**. The one at lowest field is ascribed to the quaternary and the remaining two resonances are attributed to the tertiary C atoms. ¹³C resonances referring to the phenylene rings occur in the range from 150 to 125 ppm. In the case of the osmacycloferrocenophanes **3a–h** two more peaks are detected which can be traced back to the axial (180.4–176.2 ppm) and equatorial (172.5–171.0 ppm) carbonyl ligands.

Crystal Structures of 3b, 3c, and 3e. To obtain more detailed information about the structures of the osmacycloferrocenophanes, X-ray structural investigations were performed with the examples of **3b**, **3c**, and **3e**. In Table 1 selected bond distances and angles are summarized, and the corresponding ORTEP plots with atom labeling are depicted in Figures 1–3. Four molecules are found in the monoclinic (**3b,c**) and orthorhombic (**3e**) unit cells. At approximately 1.65 Å the iron atoms are nearly equidistant from the centers of the cyclopentadienyl rings, which are almost parallel to each other with angles of δ = 178.1° (**3b**), 177.9° (**3c**), and 178.2° (**3e**) (ring center–metal–ring center). The resulting dihedral angle (tilt angle α) was found to be 2.31–(32)°, 3.77(41)°, and 2.17(30)° for **3b,c,e**. All three frameworks of the macrocycles roughly reveal a boat-shaped structure in which the phenylene building blocks including the (CH₂)_n spacers form the hull and the ferrocene and Os(CO)₄ fragments the stern and bow, respectively. Due to the different substitution patterns and the different number of CH₂ units, the boat is more or less distorted. In **3b** the two metals and the centers of the phenylene rings have nearly the same distance (8.139(2) and 8.41 Å, respectively). Both phenylene rings in **3b** deviate from a perpendicular arrangement by an

(21) Lindner, E.; Pabel, M.; Eichele, K. *J. Organomet. Chem.* **1990**, *386*, 187.

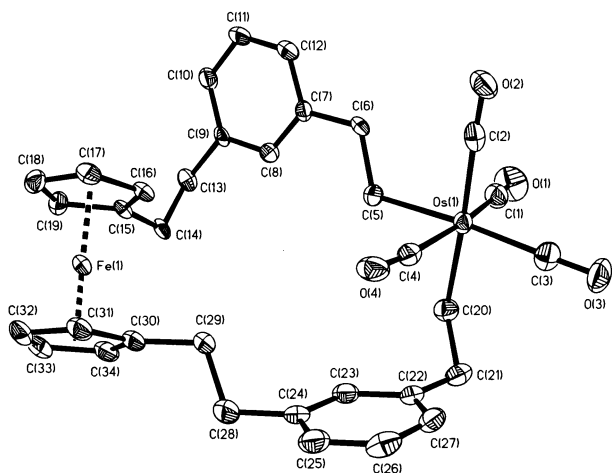


Figure 1. ORTEP plot of **3b** shown at 50% probability level; hydrogen atoms are omitted.

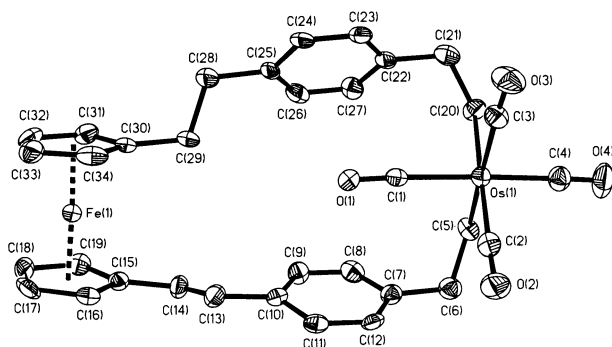


Figure 2. ORTEP plot of **3c** shown at 50% probability level; hydrogen atoms are omitted.

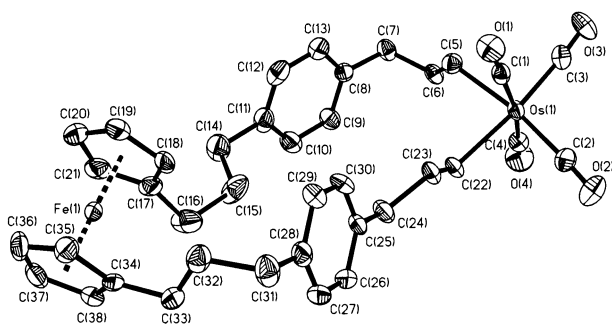


Figure 3. ORTEP plot of **3e** shown at 50% probability level; hydrogen atoms are omitted.

angle of 7.71° . For the ferrocene units a deviation of 5.7° from the synclinal (*gauche*) eclipsed (72°) conformation is established. In contrast to **3b,e** the molecule **3c** resembles most closely a boat-shaped structure. The cyclopentadienyl rings are almost eclipsed (deviation $< 0.1^\circ$), and the distances between the centers of the two phenylene groups and the metal atoms are 5.58 and $9.727(2)$ Å, respectively. The interplanar angle of the aromatic rings was found to be $53.73(17)^\circ$. At first sight the osmacycloferrocenophane **3e** is reminiscent of the diosma[7.7]paracyclophane^{11c} by replacing an $\text{Os}(\text{CO})_4$ fragment for a ferrocene unit. However, the structures of both macrocycles are rather different. The diosma[7.7]paracyclophane has C_2 symmetry, and the two phenylene functions give rise to an interplanar angle of 50.3° . Together with the metal centers they occupy the vertexes of a distorted tetrahedron (metal–metal

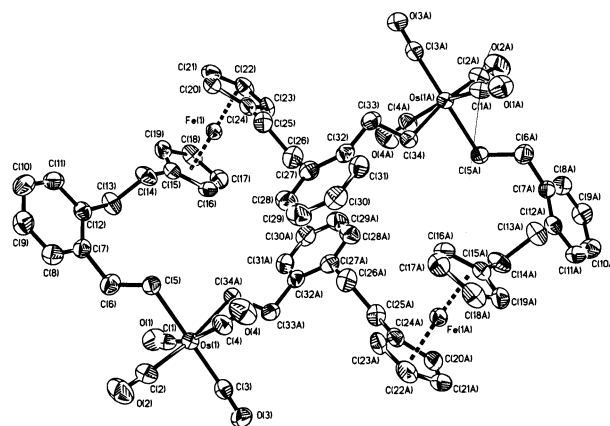


Figure 4. ORTEP plot of **4a** shown at 50% probability level; hydrogen atoms are omitted.

distance $10.07(2)$ Å). The basic cyclophane framework has a bowl-shaped structure. In the approximate boat-shaped structure of **3e** the heterometal–metal distance and the distance between the aromatic rings with interplanar angles of $27.99(24)^\circ$ are unequal ($11.468(3)$ and 6.52 Å, respectively). Like in **3b** the Cp rings in **3e** are almost in the synclinal eclipsed conformation with a deviation of 9.7° . In **3b,c,e** one carbonyl ligand is more or less bent toward the “cavity” of the respective macrocycle.

Diosmacycloferrocenophanes 4a–h. In contrast to the occurrence of only dinuclear osmaferrocenophanes,¹⁰ in the case of the osmacycloferrocenophanes not only the dinuclear species **3a–h** are formed. In reproducible yields of 1–2% (exception **4f,g** $< 0.5\%$) also the tetranuclear macrocycles **4a–h** were isolated by column chromatographic separation, eluting **3a–h** at first with *n*-pentane/diethyl ether, 50:1. It was not possible to essentially increase their yields even under optimized reaction conditions. A considerable amount of the products was insoluble in *n*-pentane, consisting of oligomeric or polymeric species. In the IR spectrum this material revealed intense CO absorptions that are characteristic of *cis*- $\text{Os}(\text{CO})_4$ fragments [IR (KBr) $\nu = 2100, 2019, 2005, 1939$ cm^{-1}]. The molecular composition of **4a–h** was corroborated by FD mass spectra. The solubility of the pale yellow heterocycles **4a–h** in nonpolar solvents such as *n*-pentane increases with the number of methylene functions. There are no significant differences in the NMR and IR data between **3a–h** and **4a–h**.

Crystal Structures of 4a and 4h. The macrocycles **4a–h** each consist of two $\text{Os}(\text{CO})_4$, $(\eta^5\text{-C}_5\text{H}_4)_2\text{Fe}$, and four *ortho*-, *meta*-, and *para*-(CH_2)_{*n*} $\text{C}_6\text{H}_4(\text{CH}_2)$ _{*n*} (*n* = 2–4), respectively. In the solid state **4a** is centrosymmetric, with four molecules in the unit cell. All four metal atoms are located at the vertexes of a distorted square with edges of $7.748(4)$ [Os(1)–Fe(1)] and $8.202(2)$ Å [Os(1)–Fe(1A)] (Figure 4). Both diagonals represent the homometal–metal distances of $11.611(5)$ [Os(1)–Os(1A)] and $10.945(3)$ Å [Fe(1)–Fe(1A)]. Referring to the ferrocene building blocks, the cyclopentadienyl rings are between a synclinal staggered (36°) and a synclinal eclipsed (72°) conformation (Figure 4). The basic cyclophane framework has roughly the shape of a part of a paddle-wheel in which the centers of the phenylene rings are placed above [C(7)–C(12)/

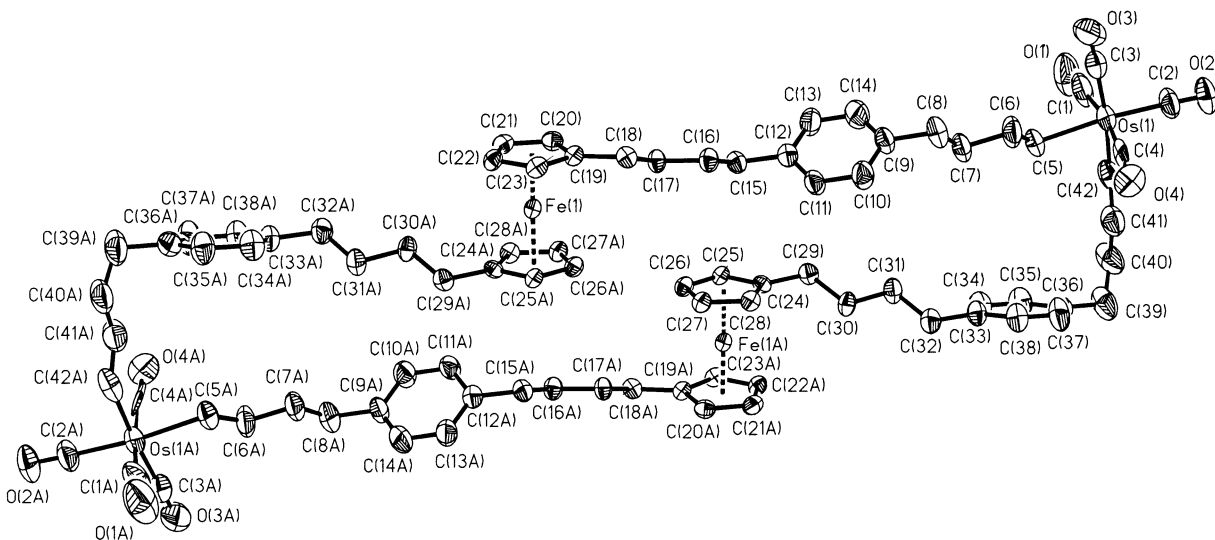


Figure 5. ORTEP plot of **4h** shown at 50% probability level; hydrogen atoms are omitted.

C(27)–C(32)] and below [C(7A)–C(12A)/C(27A)–C(32A)] the plane defined by the four metal atoms with distances of 3.54 and 2.54 Å, respectively. The distances of the phenylene rings related by the center of symmetry are 17.23 [C(7)–C(12)/C(7A)–C(12A)] and 5.35 Å [C(27)–C(32)/C(27A)–C(32A)].

Similarly the larger macrocycle **4h** is centrosymmetric and includes one molecule each of **4h** and *n*-hexane in the unit cell. In contrast to **4a** the four metal atoms are positioned at the vertexes of a parallelogram and the edges have lengths of 17.292(3) [Os(1)–Fe(1)] and 13.124(2) Å [Os(1)–Fe(1A)]. The Os(1)–Os(1A) and Fe(1)–Fe(1A) distances of 29.850(5) and 7.173(2) Å are the diagonals of this parallelogram (Figure 5). A deviation of 5.4° from the anticlinical (eclipsed) conformation (144°) is observed for the cyclopentadienyl rings in both ferrocene units, which has a significant effect on the shape of **4h**. The centers of the phenylene rings of the remarkably stretched macrocycle **4h** are above [C(9)–C(14)/C(33)–C(38)] and below [C(9A)–C(14A)/C(33A)–C(38A)] the plane defined by the four metal atoms, with distances of 0.38 and 0.79 Å, respectively. Selected bond distances and angles are depicted in Table 2.

Redox Behavior of the Bis(alcohols) 1a–h and the Macrocycles 3a–h. The redox potentials of the bis-(alcohols) **1a–h** and the osmacycloferrocenophanes **3a–h** were investigated by cyclic voltammetry with respect to the chain lengths of the (CH₂)_{*n*} spacers and the substitution patterns of the phenylene groups. All cyclic voltammograms of **1a–h** and **3a–h** recorded in acetonitrile as solvent exhibit only a single oxidation/reduction peak couple within the potential window (–1.6 to 1.6 V) and are similar in shape to the unsubstituted ferrocene (ferrocene/ferrocenium cation). Due to the peak potential separations (50–70 mV, scan rate *v* 100–10000 mV/s, theoretical: 59 mV), *i*_{pc}/*i*_{pa} ratios (1.0 ± 0.1), *i*_{pa} vs *v*^{1/2} plots (linear), and (*E*_{pa} + *E*_{pc})/2 values (constant over the entire range of the scan rate), the electrochemical and chemical reversibility could be established. If the redox potentials *E*_{1/2} of the bis-(alcohols) **1a–h** are compared to those of the corresponding osmacycloferrocenophanes **3a–h** (Table 3), only differences of the *E*_{1/2} values for **1a/3a** and **1f/3f** (*ortho*-phenylene) are significant beyond the limit of error

Table 2. Selected Bond Lengths (Å) and Bond Angles (deg) for **4a** and **4h**

	4a	4h
Os(1)–Fe(1)	7.748(4)	17.292(3)
Os(1)–Fe(1A)	8.202(2)	13.124(2)
Os(1)–Os(1A)	11.611(5)	29.850(5)
Fe(1)–Fe(1A)	10.945(3)	7.173(2)
Os(1)–C(5)	2.214(4)	2.228(8)
Os(1)–C(34A)	2.212(4)	
Os(1)–C(42)		2.193(12)
center Ph(1)–center Ph(2)	8.689	7.650
center Ph(1)–center Ph(1A)	17.23	14.09
center Ph(2)–center Ph(2A)	5.35	23.57
Fe–Cp(1)	1.64	1.66
Fe–Cp(2)	1.64	1.66
C(5)–Os(1)–C(34A)	85.17(15)	
C(5)–Os(1)–C(42)		84.0(4)
δ	177.0	178.6
α	4.5	1.8
C(14)–Cp(1)–Cp(2)–C(25)	54.2	
C(18)–Cp(1)–Cp(2)–C(29A)		149.4
interplanar angle (Ph(1)–Ph(2))	100.8	43.8

Table 3. Formal Potentials of **1a–h** and **3a–h** versus Fc/Fc⁺

compound	<i>E</i> _{1/2} , mV	Δ <i>E</i> , mV	<i>i</i> _{pc} / <i>i</i> _{pa}
1a	–83	61	0.998
1b	–88	63	1.023
1c	–95	59	0.988
1d	–98	61	1.001
1e	–105	61	1.000
1f	–108	65	1.023
1g	–104	63	1.007
1h	–110	61	1.004
3a	–72	60	0.992
3b	–87	60	1.006
3c	–89	63	1.003
3d	–101	61	0.999
3e	–102	62	1.000
3f	–93	61	1.001
3g	–103	60	1.020
3h	–110	60	1.014

of the experiment. Within this series **1a,f** are easier oxidized than **3a,f**. In the case of **1b–e,g,h** and **3b–e,g,h** nearly no difference was found whether there are OH or Os(CO)₄ groups in the molecule. Nevertheless the *E*_{1/2} values vary from –83 to –110 and –72 to –110 mV for **1a–h** and **3a–h**, respectively, indicating that **1a–h** and **3a–h** are easier oxidized than ferrocene itself. Compared to osmaferrocenophanes¹⁰ the osmacyclofer-

rocenophanes **3a–h** reveal slightly higher $E_{1/2}$ values. It seems that the inductive electron-donating effect of the $(\text{CH}_2)_2$ spacers in **1a–c** and **3a–c** is partially reduced due to the inductive electron-withdrawing effect of the phenylene groups, affecting the ferrocenes via the two methylene functions. For example the redox potentials of $1,1'\text{-fc}(\text{C}_6\text{H}_5)_2$ and $1,1'\text{-fc}(\text{CH}_2\text{C}_6\text{H}_5)_2$, which are provided with either no or one methylene group between the ferrocene and the benzene ring, are 40 and -40 mV,²² respectively. Compared to these results, the influence of the aromatic ring via the $(\text{CH}_2)_2$ spacer is small. On going from $(\text{CH}_2)_2$ to $(\text{CH}_2)_4$ via the $(\text{CH}_2)_3$ spacers, the redox potentials converge to that of diethylferrocene ($E_{1/2} = -113$ to -117 mV)²³ and higher homologues.²²

Conclusion

As already demonstrated in previous investigations, the bis(triflate) method^{10,11,17–19} is a versatile tool for the concomitant formation of several metal–carbon σ bonds. Dependent on the design of the hydrocarbon framework, the formation of macrocycles with one,^{11b,19} two,^{10,11a–c,19} or even three¹⁹ transition metal centers was observed. In the present work we applied this route to combine for the first time structural features of typical metallacyclophanes with metallocenophanes. The resulting osmacycloferrocenophanes **3a–h** and **4a–h** attract attention for their thermal stability (> 100 °C) and consist of an extended hydrocarbon skeleton containing additionally two and four transition metal centers, respectively. Macrocycles of this type not only represent aesthetic structures^{11a,c} but may also be regarded as valuable building blocks²⁴ for the synthesis of new materials with interesting properties. If in dinuclear macrocycles one transition metal fragment is replaced for a metallocene, structures may change considerably. A typical example of this observation is the comparison between the diosma[7.7]paracyclophane^{11c} and the osmacycloferrocenophane **3e**. While in the first case a bowl-shaped structure is preferred, in **3e** a boatlike framework was established.

Regarding the yields, the formation of monoosmacycloferrocenophanes **3a–h** was favored over that of the diosmacycloferrocenophanes **4a–h**. A mechanistic reflection of this fact was already described in an earlier paper.¹⁰ Mainly entropic effects²⁵ are responsible for this observation.

The cyclic voltammograms of the ferrocene derivatives **1a–h** and **3a–h** are characterized by a reversible one-electron oxidation process. However, with the exception of **1a/3a** and **1f/3f** there is no remarkable difference between the redox potentials of **1a–h** and **3a–h**. Obviously, due to the long distance between the ferrocene and the OH and Os(CO)₄ unit, respectively, the redox potentials are scarcely affected. A crucial factor for the $E_{1/2}$ values is the number of methylene functions

between the ferrocene and phenylene rings and their substitution patterns. For **1a/3a** and **1f/3f** with *ortho*-substituted aromatic rings, small differences are established between the bis(alcohols) and the corresponding osmacycloferrocenophanes.

Experimental Section

General Comments. All manipulations were carried out under an atmosphere of argon by use of standard Schlenk techniques. Solvents were dried with appropriate reagents and stored under argon. NMR spectra were recorded at 250.13 MHz (¹H NMR) and 62.90 MHz (¹³C{¹H} NMR) on a Bruker DRX 250 at 20 °C, if not stated otherwise. ¹H and ¹³C chemical shifts were measured relative to partially deuterated and deuterated solvent peaks, respectively, which are reported relative to TMS. Elemental analyses were carried out with an Elementar Vario EL analyzer. FD mass spectra were recorded on a Finnigan MAT 711 A instrument, modified by AMD, and EI mass spectra were taken on a Finnigan MAT TSQ 80. IR data were obtained with a Bruker IFS 48 FTIR spectrometer. Os₃(CO)₁₂²⁶ and Na₂[Os(CO)₄]²⁷ were synthesized according to literature methods.

General Procedure for the Preparation of the Osmacycloferrocenophanes **3a–h and Diosmacycloferrocenophanes **4a–h**.** A solution of the bis(triflates) **2a–h** (1.0 mmol) in 10 and 90 mL of diethyl and dimethyl ether at -80 °C, respectively, was added dropwise within 4 h to a suspension of Na₂[Os(CO)₄] (348.2 mg, 1.0 mmol) in 100 mL of refluxing dimethyl ether. Stirring and refluxing this mixture for 3 days afforded a yellow clear solution and a yellow-brown precipitate. After evaporation of the solvents the residue was extracted three times with 200 mL of *n*-pentane. The insoluble components were filtered off (P4), and the solvent was evaporated under reduced pressure, leaving the crude products, which were purified by column chromatography on silica gel ($l = 20$ cm, *n*-pentane/Et₂O, 50:1 (**3a–h**); *n*-pentane/Et₂O, 25:1 (**4a–h**)). Recrystallization from *n*-pentane at -80 °C afforded the analytically pure osmacycloferrocenophanes **3a–h** and diosmacycloferrocenophanes **4a–h**.

11,11,11,11-Tetracarbonyl-11-osma[2]orthocyclo[5]orthocyclo[2]-(1,1)ferrocenophane (3a**).** Yield: 113 mg (15%), yellow, air-stable crystals, mp 151 °C. ¹H NMR (CD₂Cl₂): δ 7.21–7.01 (m, 8H, CH_{arom}), 4.02 (m,²⁸ 8H, C₅H₄), 3.10 (m,²⁹ $N = 17.8$ Hz, 4H, OsCH₂CH₂C_{arom}), 2.91–2.84 (m, 4H, C₅H₄-CH₂CH₂C_{arom}), 2.70–2.64 (m, 4H, CH₂C₅H₄), 1.41 (m,³⁰ $N = 17.6$ Hz, 4H, CH₂Os). ¹³C{¹H} NMR (CD₂Cl₂): δ 180.4 (s, OsCO_{ax}), 172.5 (s, OsCO_{eq}), 147.4, 140.5 (s, C_{arom}), 131.4, 130.8, 127.7, 127.2 (s, CH_{arom}), 90.4 (s, C₄H₄O), 70.6, 68.7 (s, C₄H₄C), 42.7, 36.1, 33.6 (s, CH₂), -0.8 (s, CH₂Os). IR (*n*-pentane, cm⁻¹): ν (CO) 2124, 2045, 2035, 2012. FD-MS: m/z 752.0 [M⁺]. CV: $E_{1/2} -72$ mV. Anal. Calcd for C₃₄H₃₂FeO₄Os: C, 54.40; H, 4.30. Found: C, 54.08; H, 4.04.

11,11,11,11-Tetracarbonyl-11-osma[2]metacyclo[5]metacyclo[2]-(1,1)ferrocenophane (3b**).** Yield: 173 mg (23%), yellow, air-stable crystals, mp 122 °C. ¹H NMR (CD₂Cl₂): δ 7.21–6.94 (m, 8H, CH_{arom}), 4.03 (m,²⁸ 8H, C₅H₄), 3.03 (m,²⁹ $N = 17.9$ Hz, 4H, OsCH₂CH₂C_{arom}), 2.82–2.66 (m, 8H, CH₂C_{arom}, CH₂C₅H₄), 1.40 (m,³⁰ $N = 17.9$ Hz, 4H, CH₂Os). ¹³C{¹H} NMR (CD₂Cl₂): δ 178.2 (s, OsCO_{ax}), 171.1 (s, OsCO_{eq}), 142.8, 142.5 (s, C_{arom}), 128.2, 127.3, 125.8, 125.3 (s, CH_{arom}), 89.0 (s, C₄H₄O), 69.3, 67.3 (s, C₄H₄C), 43.6, 38.5, 32.1 (s, CH₂), 0.7 (s, CH₂Os). IR (*n*-pentane, cm⁻¹): ν (CO) 2126, 2044, 2040, 2012. FD-MS: m/z 752.0 [M⁺]. CV: $E_{1/2} -87$ mV. Anal. Calcd for C₃₄H₃₂FeO₄Os: C, 54.40; H, 4.30. Found: C, 54.37; H, 3.89.

(22) Lu, S.; Strelets, V. V.; Ryan, M. F.; Pietro, W. J.; Lever, A. B. P. *Inorg. Chem.* **1996**, *35*, 1013.

(23) (a) Hall, D. W.; Russel, C. D. *J. Am. Chem. Soc.* **1967**, *89*, 2316. (b) Fujita, E.; Gordon, B.; Hillman, M. J.; Nagy, A. G. *J. Organomet. Chem.* **1981**, *218*, 105. (c) Kuwana, T.; Bublitz, D. E.; Hoh, G. *J. Am. Chem. Soc.* **1960**, *82*, 5811.

(24) Togni, A. In *Ferrocenes*; Togni, A., Hayashi, T., Eds.; VCH: Weinheim, 1995; p 433.

(25) Illuminati, G.; Mandolini, L. *Acc. Chem. Res.* **1981**, *14*, 95.

(26) Drake, S. R.; Loveday, P. A. *Inorg. Synth.* **1991**, *28*, 230.

(27) Carter, W. J.; Kelland, J. W.; Okrasinski, S. J.; Warner, K. E.; Norton, J. R. *Inorg. Chem.* **1982**, *21*, 3955.

(28) *m*: AA'XX' pattern

(29) *m*: low-field part of an AA'XX' pattern.

(30) *m*: high-field part of an AA'XX' pattern.

11,11,11,11-Tetracarbonyl-11-osma[2]paracyclo[5]paracyclo[2]-(1,1')ferrocenophane (3c). Yield: 128 mg (17%), yellow, air-stable crystals, dec 172 °C. ¹H NMR (CD₂Cl₂): δ 7.10–7.00 (m, 8H, CH_{arom}), 4.07 (m, ²⁸ 8H, C₅H₄), 3.19–3.15 (m, 4H, OsCH₂CH₂C_{arom}), 2.56–2.49 (m, 4H, C₅H₄CH₂CH₂C_{arom}), 2.15–2.08 (m, 4H, CH₂C₅H₄), 1.30–1.26 (m, 4H, CH₂Os). ¹³C-{¹H} NMR (CD₂Cl₂): δ 176.2 (s, OsCO_{ax}), 171.4 (s, OsCO_{eq}), 142.8, 140.7 (s, C_{arom}), 128.8, 128.1 (s, CH_{arom}), 88.2 (s, C₄H₄C), 68.3, 67.2 (s, C₄H₄C), 41.2, 39.3, 33.0 (s, CH₂), 1.8 (s, CH₂Os). IR (*n*-pentane, cm⁻¹): ν(CO) 2128, 2050, 2036, 2001. FD-MS: *m/z* 751.7 [M⁺]. CV: E_{1/2} -89 mV. Anal. Calcd for C₃₄H₃₂FeO₄: C, 54.40; H, 4.30. Found: C, 54.20; H, 4.25.

13,13,13,13-Tetracarbonyl-13-osma[3]metacyclo[7]metacyclo[3]-(1,1')ferrocenophane (3d). Yield: 163 mg (20%), yellow, air-stable crystals, mp 61.3 °C. ¹H NMR (CD₂Cl₂): δ 7.21–6.97 (m, 8H, CH_{arom}), 3.93 (m, ²⁸ 8H, C₅H₄), 2.64–2.56 (m, 8H, CH₂C_{arom}), 2.28 (t, ³J_{HH} = 7.5 Hz, 4H, CH₂C₅H₄), 2.12–1.99 (m, 4H, OsCH₂CH₂CH₂C_{arom}), 1.91–1.79 (m, 4H, C₅H₄-CH₂CH₂CH₂C_{arom}), 1.01 (m, ³⁰ N = 17.0 Hz, 4H, CH₂Os). ¹³C-{¹H} NMR (CD₂Cl₂): δ 178.9 (s, OsCO_{ax}), 171.1 (s, OsCO_{eq}), 142.3 (s, C_{arom}), 128.6, 128.1, 126.0, 125.8 (s, CH_{arom}), 89.2 (s, C₄H₄C), 68.6, 67.3 (s, C₄H₄C), 42.4, 39.1, 35.6, 32.3, 28.2 (s, CH₂), -3.9 (s, CH₂Os). IR (*n*-pentane, cm⁻¹): ν(CO) 2125, 2039, 2009. FD-MS: *m/z* 808.5 [M⁺]. CV: E_{1/2} -101 mV. Anal. Calcd for C₃₈H₄₀FeO₄: C, 56.57; H, 5.00. Found: C, 56.42; H, 4.64.

13,13,13,13-Tetracarbonyl-13-osma[3]paracyclo[7]paracyclo[3]-(1,1')ferrocenophane (3e). Yield: 183 mg (23%), yellow, air-stable crystals, mp 127.5 °C. ¹H NMR (CD₂Cl₂): δ 7.14–7.06 (m, 8H, CH_{arom}), 3.95 (m, ²⁸ 8H, C₅H₄), 2.66–2.53 (m, 8H, CH₂C_{arom}), 2.32 (t, ³J_{HH} = 8.0 Hz, 4H, CH₂C₅H₄), 2.08–1.82 (m, 8H, CH₂CH₂CH₂), 0.96 (m, ³⁰ N = 17.3 Hz, 4H, CH₂-Os). ¹³C-{¹H} NMR (CD₂Cl₂): δ 178.8 (s, OsCO_{ax}), 171.0 (s, OsCO_{eq}), 139.6, 139.4 (s, C_{arom}), 128.5, 128.2 (s, CH_{arom}), 89.3 (s, C₄H₄C), 68.7, 67.1 (s, C₄H₄C), 41.6, 38.2, 35.2, 31.8, 28.0 (s, CH₂), -5.5 (s, CH₂Os). IR (*n*-pentane, cm⁻¹): ν(CO) 2125, 2040, 2009. FD-MS: *m/z* 808.4 [M⁺]. CV: E_{1/2} -102 mV. Anal. Calcd for C₃₈H₄₀FeO₄: C, 56.57; H, 5.00. Found: C, 56.31; H, 4.99.

15,15,15,15-Tetracarbonyl-15-osma[4]orthocyclo[9]orthocyclo[4]-(1,1')ferrocenophane (3f). Yield: 173 mg (20%), yellow, air-stable crystals, mp 90.3 °C. ¹H NMR (CD₂Cl₂): δ 7.16–7.08 (m, 8H, CH_{arom}), 3.97 (m, ²⁸ 8H, C₅H₄), 2.70–2.64 (m, 8H, CH₂C_{arom}), 2.37 (t, ³J_{HH} = 6.8 Hz, 4H, CH₂C₅H₄), 1.97–1.85 (m, 4H, CH₂CH₂CH₂Os), 1.67–1.51 (m, 12H, CH₂CH₂-CH₂), 1.14–1.07 (m, ²⁹ N = 17.3 Hz, 4H, CH₂Os). ¹³C-{¹H} NMR (CD₂Cl₂): δ 179.5 (s, OsCO_{ax}), 171.2 (s, OsCO_{eq}), 141.0, 140.6 (s, C_{arom}), 129.4, 129.3, 125.8, 125.7 (s, CH_{arom}), 89.2 (s, C₄H₄C), 68.7, 67.6 (s, C₄H₄C), 38.8, 38.7, 32.8, 32.4, 31.7, 31.2, 29.1 (s, CH₂), -3.2 (s, CH₂Os). IR (*n*-pentane, cm⁻¹): ν(CO) 2124, 2039, 2010. FD-MS: *m/z* 863.7 [M⁺]. CV: E_{1/2} -93 mV. Anal. Calcd for C₄₂H₄₈FeO₄: C, 58.46; H, 5.61. Found: C, 58.23; H, 5.35.

15,15,15,15-Tetracarbonyl-15-osma[4]metacyclo[9]metacyclo[4]-(1,1')ferrocenophane (3g). Yield: 226 mg (26%), yellow, air-stable crystals, mp 82.1 °C. ¹H NMR (CD₂Cl₂): δ 7.14–6.98 (m, 8H, CH_{arom}), 3.93 (m, ²⁸ 8H, C₅H₄), 2.65–2.57 (m, 8H, CH₂C_{arom}), 2.33 (t, ³J_{HH} = 7.7 Hz, 4H, CH₂C₅H₄), 1.83–1.51 (m, 16H, CH₂CH₂CH₂), 1.04 (m, ³⁰ N = 17.0 Hz, 4H, CH₂-Os). ¹³C-{¹H} NMR (CD₂Cl₂): δ 179.3 (s, OsCO_{ax}), 171.2 (s, OsCO_{eq}), 143.1, 142.7 (s, C_{arom}), 128.5, 128.1, 125.8 (s, CH_{arom}), 89.4 (s, C₄H₄C), 68.9, 67.4 (s, C₄H₄C), 38.7, 37.7, 35.7, 35.2, 31.7, 31.0, 29.3 (s, CH₂), -3.1 (s, CH₂Os). IR (*n*-pentane, cm⁻¹): ν(CO) 2125, 2040, 2008. FD-MS: *m/z* 863.7 [M⁺]. CV: E_{1/2} -103 mV. Anal. Calcd for C₄₂H₄₈FeO₄: C, 58.46; H, 5.61. Found: C, 58.31; H, 5.21.

15,15,15,15-Tetracarbonyl-15-osma[4]paracyclo[9]paracyclo[4]-(1,1')ferrocenophane (3h). Yield: 232 mg (27%), yellow, air-stable crystals, mp 73.3 °C. ¹H NMR (CD₂Cl₂): δ 7.09 (s, 8H, CH_{arom}), 3.89 (m, ²⁸ 8H, C₅H₄), 2.63–2.57 (m, 8H, CH₂C_{arom}), 2.25 (t, ³J_{HH} = 7.7 Hz, 4H, CH₂C₅H₄), 1.72–1.46 (m, 16H, CH₂CH₂CH₂), 0.97–0.91 (m, 4H, CH₂Os). ¹³C-{¹H} NMR (CD₂Cl₂): δ 179.0 (s, OsCO_{ax}), 171.2 (s, OsCO_{eq}), 140.1, 139.7 (s, C_{arom}), 128.5, 128.3 (s, CH_{arom}), 89.4 (s, C₄H₄C), 68.5,

67.2 (s, C₄H₄C), 37.6, 36.5, 35.1, 34.2, 31.4, 29.9, 28.7 (s, CH₂), -4.0 (s, CH₂Os). IR (*n*-pentane, cm⁻¹): ν(CO) 2125, 2040, 2008. FD-MS: *m/z* 863.7 [M⁺]. CV: E_{1/2} -110 mV. Anal. Calcd for C₄₂H₄₈FeO₄: C, 58.46; H, 5.61. Found: C, 58.53; H, 5.61.

11,11,11,11,43,43,43,43-Octacarbonyl-11,43-diosma[2]-orthocyclo[5]orthocyclo[2]-(1,1')ferroceno[2]orthocyclo[5]orthocyclo[2]-(1,1')ferrocenophane (4a). Yield: 17 mg (2%), pale yellow, air-stable crystals, mp 152 °C. ¹H NMR (CD₂-Cl₂): δ 7.15–7.09 (m, 16H, CH_{arom}), 3.93 (s, 16H, C₅H₄), 2.95 (m, ²⁹ N = 17.9 Hz, 8H, OsCH₂CH₂C_{arom}), 2.91–2.84 (m, 8H, C₅H₄CH₂CH₂C_{arom}), 2.61–2.54 (m, 8H, CH₂C₅H₄), 1.24 (m, ³⁰ N = 17.9 Hz, 8H, CH₂Os). ¹³C-{¹H} NMR (CD₂Cl₂): δ 179.1 (s, OsCO_{ax}), 171.0 (s, OsCO_{eq}), 146.0, 139.0 (s, C_{arom}), 129.3, 128.7, 126.2, 125.7 (s, CH_{arom}), 88.5 (s, C₄H₄C), 68.6, 68.1 (s, C₄H₄C), 41.3, 34.5, 31.7 (s, CH₂), -1.4 (s, CH₂Os). IR (*n*-pentane, cm⁻¹): ν(CO) 2124, 2045, 2038, 2012. FD-MS: *m/z* 1496 (5%), 1497 (15%), 1498 (53%), 1499 (61%), 1500 (76%), 1501 (83%), 1502 (100%), 1503 (86%), 1504 (58%), 1505 (35%), 1506 (10%); calcd 1496 (14%), 1497 (25%), 1498 (47%), 1499 (58%), 1500 (82%), 1501 (82%), 1502 (100%), 1503 (62%), 1504 (63%), 1505 (39%), 1506 (15%) [M⁺ (isotopic distribution)]. Anal. Calcd for C₆₈H₆₄-Fe₂O₈Os₂: C, 54.40; H, 4.30. Found: C, 54.22; H, 4.35.

11,11,11,11,43,43,43,43-Octacarbonyl-11,43-diosma[2]-metacyclo[5]metacyclo[2]-(1,1')ferroceno[2]metacyclo[5]-metacyclo[2]-(1,1')ferrocenophane (4b). Yield: 7 mg (1%), pale yellow, air-stable crystals, mp 124 °C. ¹H NMR (CD₂Cl₂): δ 7.21–6.96 (m, 16H, CH_{arom}), 3.98 (m, ²⁸ 16H, C₅H₄), 2.96 (m, ²⁹ N = 17.6 Hz, 8H, OsCH₂CH₂C_{arom}), 2.79–2.73 (m, 8H, C₅H₄-CH₂CH₂C_{arom}), 2.63–2.56 (m, 8H, CH₂C₅H₄), 1.30–1.20 (m, 8H, CH₂Os). ¹³C-{¹H} NMR (CD₂Cl₂): δ 178.8 (s, OsCO_{ax}), 171.0 (s, OsCO_{eq}), 148.2, 142.4 (s, C_{arom}), 128.2, 127.9, 125.6, 125.3 (s, CH_{arom}), 88.7 (s, C₄H₄C), 68.8, 67.8 (s, C₄H₄C), 44.1, 37.7, 31.7 (s, CH₂), -0.7 (s, CH₂Os). IR (*n*-pentane, cm⁻¹): ν(CO) 2125, 2045, 2039, 2011. FD-MS: *m/z* 1496 (20%), 1497 (15%), 1498 (39%), 1499 (45%), 1500 (66%), 1501 (63%), 1502 (100%), 1503 (62%), 1504 (57%), 1505 (23%), 1506 (8%); Calcd 1496 (14%), 1497 (25%), 1498 (47%), 1499 (58%), 1500 (82%), 1501 (82%), 1502 (100%), 1503 (62%), 1504 (63%), 1505 (39%), 1506 (15%) [M⁺ (isotopic distribution)].³¹

11,11,11,11,43,43,43,43-Octacarbonyl-11,43-diosma[2]-paracyclo[5]paracyclo[2]-(1,1')ferroceno[2]paracyclo[5]-paracyclo[2]-(1,1')ferrocenophane (4c). Yield: 16 mg (2%), pale yellow, air-stable crystals, mp 163 °C. ¹H NMR (CD₂Cl₂): δ 7.14–7.07 (m, 16H, CH_{arom}), 3.99 (m, ²⁸ 16H, C₅H₄), 2.97 (m, ²⁹ N = 17.9 Hz, 8H, OsCH₂CH₂C_{arom}), 2.79–2.71 (m, 8H, C₅H₄-CH₂CH₂C_{arom}), 2.66–2.60 (m, 8H, CH₂C₅H₄), 1.30–1.20 (m, ³⁰ N = 17.9 Hz, 8H, CH₂Os). ¹³C-{¹H} NMR (CD₂Cl₂): δ 178.7 (s, OsCO_{ax}), 171.0 (s, OsCO_{eq}), 145.8, 139.5 (s, C_{arom}), 128.3, 127.6 (s, CH_{arom}), 88.9 (s, C₄H₄C), 68.9, 67.5 (s, C₄H₄C), 43.8, 37.3, 31.7 (s, CH₂), -0.7 (s, CH₂Os). IR (*n*-pentane, cm⁻¹): ν(CO) 2128, 2050, 2036, 2001. FD-MS: *m/z* 1496 (16%), 1497 (36%), 1498 (55%), 1499 (78%), 1500 (85%), 1501 (80%), 1502 (100%), 1503 (50%), 1504 (77.3%), 1505 (47%), 1506 (15%); calcd 1496 (14%), 1497 (25%), 1498 (47%), 1499 (58%), 1500 (82%), 1501 (82%), 1502 (100%), 1503 (62%), 1504 (63%), 1505 (39%), 1506 (15%) [M⁺ (isotopic distribution)]. Anal. Calcd for C₆₈H₆₄Fe₂O₈Os₂: C, 54.40; H, 4.30. Found: C, 54.10; H, 3.93.

13,13,13,13,49,49,49,49-Octacarbonyl-13,49-diosma[3]-metacyclo[7]metacyclo[3]-(1,1')ferroceno[3]metacyclo[7]-metacyclo[3]-(1,1')ferrocenophane (4d). Yield: 10 mg (1%), pale yellow, air-stable crystals, mp 60.4 °C. ¹H NMR (CD₂-Cl₂): δ 7.21–6.98 (m, 16H, CH_{arom}), 3.95 (m, ²⁸ 16H, C₅H₄), 2.63–2.53 (m, 16H, CH₂C_{arom}), 2.37–2.28 (m, 8H, CH₂C₅H₄), 2.09–1.96 (m, 8H, CH₂CH₂CH₂), 1.88–1.75 (m, 8H, CH₂CH₂-CH₂), 1.04 (m, ³⁰ N = 17.0 Hz, 8H, CH₂Os). ¹³C-{¹H} NMR (CD₂-Cl₂): δ 179.2 (s, OsCO_{ax}), 171.0 (s, OsCO_{eq}), 142.6, 142.5 (s, C_{arom}), 128.7, 128.1, 125.8, 125.7 (s, CH_{arom}), 89.0 (s, C₄H₄C), 68.6, 67.7 (s, C₄H₄C), 43.0, 40.6, 35.8, 32.8, 28.8 (s, CH₂), -3.2 (s, CH₂Os). IR (*n*-pentane, cm⁻¹): ν(CO) 2125, 2039, 2009. FD-

(31) Due to the very low yield, no elemental analyses were available.

Table 4. Crystal Data and Summary of Data Collection and Refinement for 3b, 3c, 3e, 4a, and 4h

	3b	3c ·0.5CH ₂ Cl ₂	3e	4a	4h · <i>n</i> -hexane
formula	C ₃₄ H ₃₂ FeO ₄ Os	C _{34.5} H ₃₃ ClFeO ₄ Os	C ₃₈ H ₄₀ FeO ₄ Os	C ₆₈ H ₆₄ Fe ₂ O ₈ Os ₂	C ₉₀ H ₁₁₀ Fe ₂ O ₈ Os ₂
fw	750.65	793.11	806.75	1501.29	1811.88
cryst size, mm ³	0.25 × 0.45 × 0.25	0.6 × 0.15 × 0.04	0.2 × 0.6 × 0.4	0.50 × 0.40 × 0.10	0.5 × 0.08 × 0.08
temp, K	173(2)	173(2)	173(2)	173(2)	173(2)
cryst syst	monoclinic	monoclinic	orthorhombic	orthorhombic	triclinic
space group	<i>P</i> 2 ₁ / <i>n</i>	<i>P</i> 2 ₁ / <i>n</i>	<i>P</i> 2 ₁ 2 ₁ 2 ₁	<i>Pbca</i>	<i>P</i> $\bar{1}$
<i>a</i> , Å	6.195(3)	6.2833(17)	8.857(2)	14.646(4)	6.6774(19)
<i>b</i> , Å	41.882(12)	16.437(3)	11.944(3)	12.629(7)	11.1945(16)
<i>c</i> , Å	11.053(3)	29.161(4)	31.810(8)	32.278(9)	29.219(4)
α , deg					93.038(8)
β , deg	95.84(3)	92.244(17)			92.63(2)
γ , deg					104.982(9)
<i>V</i> , Å ³	2852.9(18)	3009.4(10)	3365.0(15)	5970(4)	2102.9(7)
<i>Z</i>	4	4	4	4	1
<i>d</i> _{calcd} , g/cm ³	1.748	1.750	1.592	1.670	1.431
μ (Mo K α), mm ⁻¹	4.996	4.827	4.242	4.774	3.402
<i>F</i> (000), e	1480	1564	1608	2960	918
θ range, deg	2.09–27.52	2.44–27.50	2.13–27.52	2.22–27.52	2.06–27.50
index ranges	–8 ≤ <i>h</i> ≤ 8 –54 ≤ <i>k</i> ≤ 54 –14 ≤ <i>l</i> ≤ 14	–1 ≤ <i>h</i> ≤ 6 –21 ≤ <i>k</i> ≤ 1 –37 ≤ <i>l</i> ≤ 37	–4 ≤ <i>h</i> ≤ 11 –15 ≤ <i>k</i> ≤ 15 –10 ≤ <i>l</i> ≤ 41	–19 ≤ <i>h</i> ≤ 19 –16 ≤ <i>k</i> ≤ 16 –1 ≤ <i>l</i> ≤ 41	–8 ≤ <i>h</i> ≤ 1 –14 ≤ <i>k</i> ≤ 14 –37 ≤ <i>l</i> ≤ 37
no. of data collected	22663	8653	15908	26143	12141
max./min. transmn	0.7262/0.3184		0.8199/0.3536	0.762/0.362	
<i>R</i> _{int}	0.0773	0.0470	0.0355	0.0585	0.0430
no. of unique data/ restraints/params	6100/0/362	6264/2/374	7715/0/398	6587/0/362	9664/14/446
GOF on <i>F</i> ²	1.192	1.007	1.072	1.013	1.018
<i>R</i> 1, <i>wR</i> 2 (<i>I</i> > 2 σ (<i>I</i>)) ^a	0.0361, 0.0839	0.0463, 0.0974	0.0273, 0.0668	0.0308, 0.0685	0.0666, 0.1363
<i>R</i> 1, <i>wR</i> 2 (all data)	0.0430, 0.0902	0.0758, 0.1091	0.0296, 0.0678	0.0500, 0.0756	0.1299, 0.1621
largest diff peak, hole, e ⁻ /Å ³	1.832, –1.901	1.719, –1.731	1.198, –1.037	0.825, –0.949	2.061, –1.243
Flack param			–0.010(7)		

$$^a R1 = \sum(|F_o| - |F_c|)/\sum|F_o|; wR2 = [\sum[w(F_o^2 - F_c^2)^2]]^{0.5}; w = [\exp(5(\sin^2 \theta/\lambda^2))/(\sigma^2(F_o^2) + bP + (aP)^2)]; P = [F_o^2 + 2 F_c^2]/3.$$

MS: *m/z* 1608 (15%), 1609 (27%), 1610 (52%), 1611 (59%), 1612 (76%), 1613 (81%), 1614 (100%), 1615 (61%), 1616 (49%), 1617 (25%), 1618 (15%); Calcd 1608 (14%), 1609 (24%), 1610 (45%), 1611 (58%), 1612 (81%), 1613 (83%), 1614 (100%), 1615 (66%), 1616 (64%), 1617 (41%), 1618 (18%) [*M*⁺ (isotopic distribution)].³¹

13,13,13,13,49,49,49,49-Octacarbonyl-13,49-diosma[3]-paracyclo[7]paracyclo[3]-(1,1')ferroceno[3]paracyclo[7]-paracyclo[3]-(1,1')ferrocenophane (4e). Yield: 15 mg (2%), pale yellow, air-stable crystals, mp 127 °C. ¹H NMR (CD₂Cl₂): δ 7.09 (s, 16H, CH_{arom}), 3.93 (m, ²⁷16H, C₅H₄), 2.61–2.52 (m, 16H, CH₂C_{arom}), 2.28 (t, ³*J*_{HH} = 7.85 Hz, 8H, CH₂C₅H₄), 2.07–1.94 (m, 8H, CH₂CH₂CH₂), 1.85–1.73 (m, 8H, CH₂CH₂CH₂), 1.30–1.20 (m, ³⁰*N* = 17.9 Hz, 8H, CH₂Os). ¹³C{¹H} NMR (CD₂-Cl₂): δ 179.2 (s, OsCO_{ax}), 171.1 (s, OsCO_{eq}), 139.9, 139.6 (s, C_{arom}), 128.3 (s, CH_{arom}), 89.1 (s, C₄H₄C), 68.7, 67.5 (s, C₄H₄C), 42.5, 40.5, 35.3, 32.6, 28.6 (s, CH₂), –3.3 (s, CH₂Os). IR (*n*-pentane, cm⁻¹): ν (CO) 2125, 2039, 2009. FD-MS: *m/z* 1608 (20%), 1609 (33%), 1610 (65%), 1611 (62%), 1612 (89%), 1613 (61%), 1614 (100%), 1615 (73%), 1616 (38%), 1617 (29%), 1618 (14%); Calcd 1608 (14%), 1609 (24%), 1610 (45%), 1611 (58%), 1612 (81%), 1613 (83%), 1614 (100%), 1615 (66%), 1616 (64%), 1617 (41%), 1618 (18%) [*M*⁺ (isotopic distribution)]. Anal. Calcd for C₇₆H₈₀Fe₂O₈Os₂: C, 56.57; H, 5.00. Found: C, 56.63; H, 4.74.

15,15,15,15,55,55,55,55-Octacarbonyl-15,55-diosma[4]-orthocyclo[9]orthocyclo[4]-(1,1')ferroceno[4]orthocyclo[9]orthocyclo[4]-(1,1')ferrocenophane (4f). Yield < 0.5%. IR (*n*-pentane, cm⁻¹): ν (CO) 2124, 2039, 2011. FD-MS: *m/z* 1720 (17%), 1721 (23%), 1722 (47%), 1723 (66%), 1724 (85%), 1725 (87%), 1726 (100%), 1727 (57%), 1728 (55%), 1729 (36%), 1730 (15%); Calcd 1720 (13%), 1721 (24%), 1722 (44%), 1723 (57%), 1724 (80%), 1725 (84%), 1726 (100%), 1727 (70%), 1728 (65%), 1729 (44%), 1730 (20%) [*M*⁺ (isotopic distribution)].^{31,32}

(32) Due to the very low yield, no ¹H and ¹³C{¹H} NMR spectroscopic characterization was possible.

15,15,15,15,55,55,55,55-Octacarbonyl-15,55-diosma[4]-metacyclo[9]metacyclo[4]-(1,1')ferroceno[4]-metacyclo[9]-orthocyclo[4]-(1,1')ferrocenophane (4g). Yield < 0.5%. IR (*n*-pentane, cm⁻¹): ν (CO) 2124, 2039, 2009. FD-MS: *m/z* 1720 (22%), 1721 (21%), 1722 (44%), 1723 (55%), 1724 (73%), 1725 (87%), 1726 (100%), 1727 (54%), 1728 (46%), 1729 (36%), 1730 (18%); Calcd 1720 (13%), 1721 (24%), 1722 (44%), 1723 (57%), 1724 (80%), 1725 (84%), 1726 (100%), 1727 (70%), 1728 (65%), 1729 (44%), 1730 (20%) [*M*⁺ (isotopic distribution)].^{31,32}

15,15,15,15,55,55,55,55-Octacarbonyl-15,55-diosma[4]-paracyclo[9]paracyclo[4]-(1,1')ferroceno[4]paracyclo[9]-paracyclo[4]-(1,1')ferrocenophane (4h). Yield: 15 mg (2%), pale yellow, air-stable crystals, mp 65 °C. ¹H NMR (CD₂Cl₂): δ 7.09 (s, 16H, CH_{arom}), 3.93 (m, ²⁸16H, C₅H₄), 2.59 (t, ³*J*_{HH} = 7.54 Hz, 16H, CH₂C_{arom}), 2.31 (t, ³*J*_{HH} = 7.54 Hz, 8H, CH₂C₅H₄), 1.85–1.53 (m, 32H, CH₂CH₂CH₂), 1.04–0.98 (m, 8H, CH₂Os). ¹³C{¹H} NMR (CD₂Cl₂): δ 179.5 (s, OsCO_{ax}), 171.2 (s, OsCO_{eq}), 140.4, 139.9 (s, C_{arom}), 128.3 (s, CH_{arom}), 89.4 (s, C₄H₄C), 68.7, 67.5 (s, C₄H₄C), 38.6, 38.2, 35.3, 35.0, 31.6, 30.8, 29.1 (s, CH₂), –3.1 (s, CH₂Os). IR (*n*-pentane, cm⁻¹): ν (CO) 2124, 2039, 2009. FD-MS: *m/z* 1720 (15%), 1721 (25%), 1722 (34%), 1723 (77%), 1724 (87%), 1725 (92%), 1726 (100%), 1727 (60%), 1728 (52%), 1729 (40%), 1730 (5%); Calcd 1720 (13%), 1721 (24%), 1722 (44%), 1723 (57%), 1724 (80%), 1725 (84%), 1726 (100%), 1727 (70%), 1728 (65%), 1729 (44%), 1730 (20%) [*M*⁺ (isotopic distribution)]. Anal. Calcd for C₈₄H₉₆Fe₂O₈Os₂: C, 58.46; H, 5.23.

Crystallographic Analysis. Single crystals of **3b**, **3c**, **3e**, **4a**, and **4h** suitable for X-ray diffraction were obtained by slow diffusion of *n*-hexane and toluene into a solution of **3b,c,e** or **4a,h** in dichloromethane and slow evaporation of dichloromethane. Selected crystals were mounted on a P4 Siemens four-circle diffractometer. Graphite-monochromated Mo K α radiation (λ = 0.71073 Å) was used for the measurement of intensity data in the ω -scan mode. An empirical absorption correction was applied for **3b**, **3e**, and **4a** but not for **3c** and

4h. All structures were solved by direct methods with the SHELXS-86 program.³³ Refinement was carried out with full-matrix least-squares methods based on F^2 in SHELXL-97³⁴ with anisotropic thermal parameters for all non-hydrogen atoms. Hydrogen atoms were included at calculated positions using a riding model. In **3c**, the asymmetric unit contains half a molecule of dichloromethane that is disordered about the center of inversion and was included in the refinement using isotropic thermal parameters. In **4h** the unit cell contains an additional *n*-hexane molecule disordered about the center of inversion and ill defined. It was included in the refinement using isotropic thermal parameters and C–C distance restraints. Crystal data and a summary of data collection and refinement details are given in Table 4.

Electrochemical Experiments. Cyclic voltammograms were recorded with a Bioanalytical Systems (BAS, West Lafayette, IN) CV-50 W electrochemical workstation. A Metrohm Pt electrode tip (Filderstadt, Germany) was used as a working electrode. The counter electrode was a Pt wire of 1

mm diameter. A single-unit Haber-Luggin double reference electrode³⁵ was used. The resulting potential values refer to Ag/Ag⁺ (0.01 M in CH₃CN/0.1 M NBu₄PF₆). Ferrocene was used as an external standard. Its potential was determined by separate cyclic voltammetric experiments in acetonitrile. All potentials in the present paper are reported relative to the fc/fc⁺ standard.³⁶ A gastight full-glass three-electrode cell was used; its assembly has been described elsewhere.³⁷ The cell was purged with argon before it was filled with electrolyte. NBu₄PF₆ (0.1 M) was used as supporting electrolyte. Background curves were recorded before adding substrate to the solution and subtracted from the experimental data. The automatic BAS CV-50W *iR*-drop compensation facility was used for all experiments.

Acknowledgment. Support of this research by the Deutsche Forschungsgemeinschaft and the Fonds der Chemischen Industrie is gratefully acknowledged. The Degussa AG is thanked for supplying starting materials.

Supporting Information Available: Synthesis of starting materials, further details of X-ray structural determinations, including bond distances and angles and thermal parameters, for **3b**, **3c**, **3e**, **4a**, and **4h**. This material is available free of charge via the Internet at <http://pubs.acs.org>.

OM020310L

(33) Sheldrick, G. M. *SHELXLS-86*; University of Göttingen, 1986.

(34) Sheldrick, G. M. *SHELXL-97*; University of Göttingen, 1997.

(35) Gollas, B.; Krauss, B.; Speiser, B.; Stahl, H. *Curr. Sep.* **1994**, 13, 42.

(36) Gritzner, G.; Kuta, J. *Pure Appl. Chem.* **1984**, 56, 462.

(37) Dümmling, S.; Eichhorn, E.; Schneider, S.; Speiser, B.; Würde, M. *Curr. Sep.* **1996**, 15, 53.